ISSN 1087-6596, Glass Physics and Chemistry, 2015, Vol. 41, No. 5, pp. 453–459. © Pleiades Publishing, Ltd., 2015.

Short-Range Order of Germanium Selenide Glass[1]

A. H. Moharram

Rabigh College of Science and Arts, King Abdulaziz University, Rabigh 21911, Saudi Arabia
e-mail: mohar200@yahoo.com

Received December 11, 2013

Abstract—Chalcogenide $Ge_{20}Se_{80}$ glass was prepared using the melt-quench technique. The radial distribution function is obtained from X-ray diffraction data in the scattering vector interval $0.28 \le K \le 6.87$ Å^{-1}. Reverse Monte Carlo (RMC) simulations are useful to compute the partial pair distribution functions, $g_{ij}(r)$, partial structure factors, $S_{ij}(K)$, and total structure factor. Values of r_1/r_2 ratio and bond angle (Θ) indicate that $Ge(Se_{½})_4$ tetrahedra units connected by chains of the chalcogen atoms are present. The partial structure factors have shown that homopolar Ge–Ge and Se–Se bonds are behind the appearance of the first sharp diffraction peak in the total structure factor. Tetrahedral $Ge(Se_{½})_4$ structural units connected by Se-Se chains have been confirmed by the simulated values of the partial coordination numbers and the bond angle distributions. Finally, Raman spectra measurements have strongly supported the conclusions obtained either from the calculated Fourier data or from RMC simulations.

Keywords: chalcogenides, X-ray diffraction, short-range order, medium-range order, reverse Monte Carlo simulation

DOI: 10.1134/S1087659615050090

INTRODUCTION

Chalcogenide glasses present a great potential for application in technological devices, such as optical fibers, memory materials and switching devices, but their use is limited due to several factors. One of them is the difficulty in obtaining information about atomic structures. The structure of chalcogenide glasses in the short-range order (SRO) or intermediate-range order (IRO) is an important and controversial subject. The appearance of the first sharp diffraction peak (FSDP) in the total structure factor indicates the presence of IRO. Germanium selenides have been intensively studied by several methods like X-ray diffraction [1–3], Neutron diffraction [4, 5], Raman scattering [6], Anomalous X-ray scattering [7] and extended X-ray absorption fine structure (EXAFS) [8]. The structure unit in these glasses is $Ge(Se_{½})_4$ tetrahedra connected through Se chains.

As mentioned earlier [9], addition of germanium into the polymeric Se matrix produces a cross-linking of selenium chains, mediated by the formation of $Ge(Se_{1/2})_4$ tetrahedra. At low doping ($x < 15$ at %), the tetrahedra are sparsely distributed in the background matrix, with rather flexible interconnections. The feeble Ge–Ge correlations are inadequate to give any detectable FSDP, as also concluded from the partial pair structure studies on $GeSe_2$ [10]. By $x = 15$ at %, the amount of Ge becomes sufficient to join some of the tetrahedral pairs by corner sharing [11]. X-ray diffraction study of the glassy Ge_xSe_{1-x} systems [3, 7], in a wide concentration range $0 \le x \le 0.33$, have demonstrated that besides the well established SRO information, a pre-peak appeared in the total structure factor $S(K)$ at a scattering vector K of about 1.1 Å^{-1}. The pre-peak, being clear evidence for existence of the intermediate range order (IRO), showed a systematic decrease in intensity and shifts towards higher K values with decreasing Ge concentration. A similar variation in the pre-peak of the structure factor with Ge content was also observed using the neutron diffraction measurement [5].

Reverse Monte Carlo (RMC) simulation [12, 13] represents, when used carefully, a powerful tool to extract some information of intermediate and extended-range scale in glassy materials. It assembles three-dimensional atomic configurations using experimental diffraction data implicitly in the simulation. The intimate connection between computational and experimental processes means that the better quality and higher resolution of the experimental data, the more reliable RMC model of a network structure for vitreous materials. The RMC method is an inverse problem in which the experimental data are enforced to build atomic configurations that have the desired structural and electronic properties. The main point is to set up a generalized function containing as much information as possible, and then optimize the func-

[1] The article is published in the original.

tion for generating configurations toward exact agreement with the experimental data.

THEORETICAL BACKGROUND

Conventional (Fourier) Method

According to Faber and Ziman [14], the total structure factor $S(K)$ is obtained from the normalized coherent scattered intensity $I_c(K)$ through

$$S(K) = \frac{I_c(K) - \left(\left\langle f^2(K)\right\rangle - \left\langle f(K)\right\rangle^2\right)}{\left\langle f(K)\right\rangle^2}, \quad (1)$$

where $K = 4\pi(\sin\theta/\lambda)$ is the transferred momentum, $\langle f\rangle^2 = \sum_i (c_i f_i)^2$ and $\langle f^2\rangle = \sum_i c_i f_i^2$, where c_i is the atomic fraction of element i, and $f(K)$ is the atomic scattering factor.

Fourier transformation of the $S(K)$ data into real space [15] gives the reduced distribution function, $G(r)$, as follows

$$G(r) = 4\pi r[\rho(r) - \rho_0] = (2/\pi)\int_0^\infty K[S(K) - 1]M(K)\sin(Kr)dK, \quad (2)$$

where $\rho(r)$ is the local atomic density at a distance r, ρ_0 is the bulk atomic density, and $M(K)$ is called the damping factor [15, 16]. At short distances ($r \le 2$ Å), see Eq. (2), $G(r)$ should follow the density line ($-4\pi r\rho_0$) which is used as a quality check of the data. The radial distribution function, defined as the number of atoms lying at distances between r, $r + dr$ from center of an arbitrary origin atom, is given by

$$RDF(r) = 4\pi r^2\rho(r) = rG(r) + 4\pi r^2\rho_0. \quad (3)$$

The positions of the first and the second peak in the $RDF(r)$ represent the average values of the first- and second–nearest neighbor distances r_1, and r_2, respectively. A knowledge of both immediately yields a value for the bond angle $\theta = 2\sin^{-1}(r_2/2r_1)$ [5]. The area under the peak gives the corresponding coordination number.

REVERSE MONTE CARLO (RMC) METHOD

In the structural analysis using Fourier transformations [15, 17], a modification factor was suggested to reduce the effect of termination data at a finite K_{max}. This factor in turn, while reduces the spurious oscillations, leads to a broadening of the genuine peaks in $g(r)$. The broadening is wide enough to cause an overlap between the first and second peaks, and consequently introduces significant errors in the obtained structural parameters. One of the main difficulties in the study of glasses and other disordered materials is the production of structural models that agree quantitatively with diffraction date. In normal Monte Carlo simulation, an initial structure is allowed to rearrange in such a way that its energy is minimized. The RMC does not need the inter-atomic potentials and a structural configuration is adjusted so as to minimize instead the difference between the calculated diffraction pattern and that measured experimentally [18].

Three-dimensional arrangement of N atoms is placed into a cubic cell with periodic boundary conditions. The atomic number density (ρ) should be the same as the experimental value. The positions of the atoms are chosen randomly. The partial pair distribution function [12, 19] can be calculated from the initial configuration by

$$g_{ij}^{Co}(r) = \frac{n_{ij}(r)}{4\pi r^2 \mathrm{d}r\rho c_i}, \quad (4)$$

where the superscripts "C" and "o" mean "calculate" and "old", respectively, c_i is the concentration of atoms type i and $n_{ij}(r)$ is the average number of atoms type j located at distance between r and $r + \mathrm{d}r$ from a central atom of type i. Fourier transform of $g_{ij}^{Co}(r)$ to reciprocal space yields the partial static structure factor

$$S_{ij}^{Co}(K) = \rho\int_0^\infty 4\pi r^2\left(g_{ij}^{Co}(r) - 1\right)\frac{\sin Kr}{Kr}\mathrm{d}r, \quad (5)$$

where $K = 4\pi\sin\theta/\lambda$ is the momentum transfer. The total structure factor is calculated as follows

$$S^{Co}(K) = \sum_{i,j} c_i c_j f_i(K) f_j(K)\left(S_{ij}^{Co}(K) - 1\right), \quad (6)$$

where $f_i(K)$ is the atomic scattering factor of atom type i. The difference between the experimental total structure factor, $S^E(K)$, and that calculated from the configuration is given by

$$\chi_o^2 = \sum_{i=i}^{m}\left(S^{Co}(K_i) - S^E(K_i)\right)^2 \Big/ \sigma^2(K_i), \quad (7)$$

where the sum is taken over the m experimental points and σ represents the experimental error. One atom moves at random but if it approaches another atom closer than the cut-off distance, the move is rejected. Otherwise, a new atom is chosen with acceptable move. Then, the new values of the partial pair distribution functions, partial structure factors, and the total structure factor can be calculated. The new value of $S^{Cn}(K)$ gives a new difference

$$\chi_n^2 = \sum_{i=i}^{m}\left(S^{Cn}(K_i) - S^E(K_i)\right)^2 \Big/ \sigma^2(K_i), \quad (8)$$

where n means 'new'. If $\chi_n^2 < \chi_o^2$, the move is accepted and the new configuration becomes the old one. If $\chi_n^2 > \chi_o^2$, it is accepted with probability

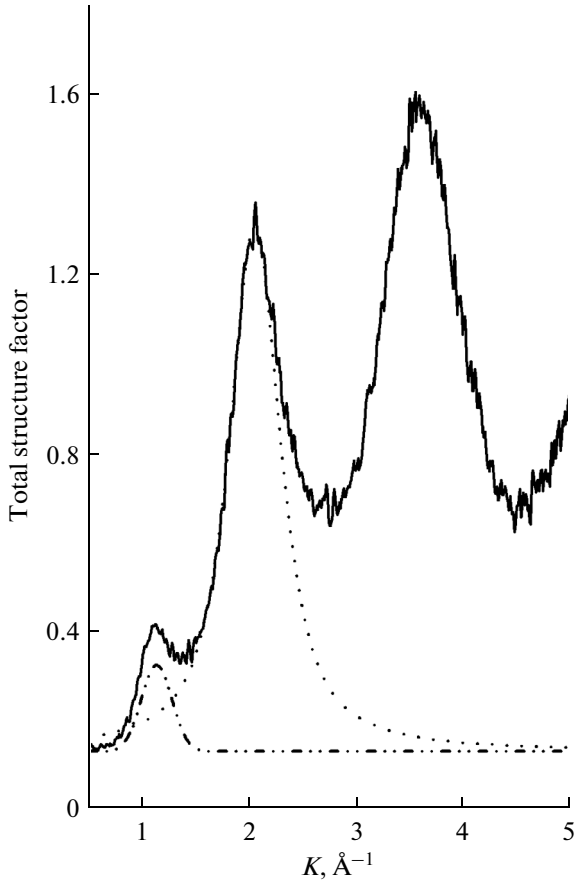

Fig. 1. The total structure factor of the $Ge_{20}Se_{80}$ glass as a function of the scattering vector (K). The spectra was analyzed using two pseudo-Voigt functions for the pre- and first-peaks.

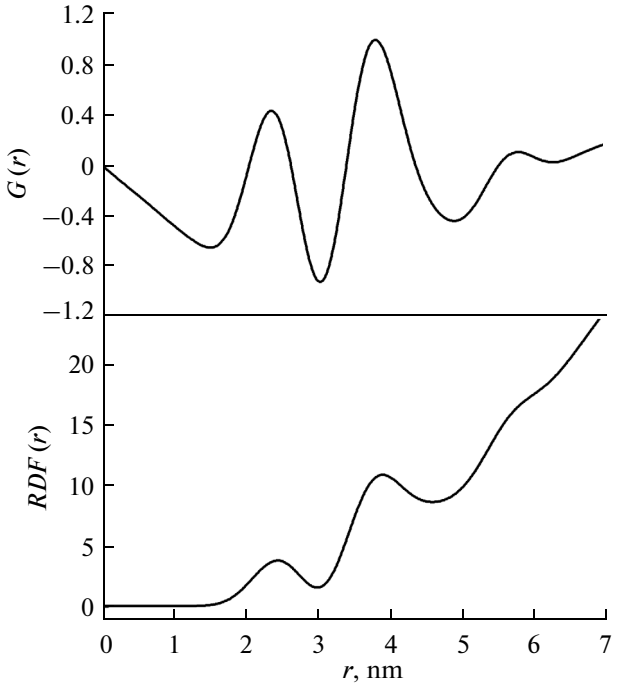

Fig. 2. The reduced distribution function, $G(r)$, and the radial distribution function, RDF(r), versus r of the investigated $Ge_{20}Se_{80}$ glass.

$\exp\left(-\left(\chi_n^2 - \chi_o^2\right)/2\right)$. Otherwise it is rejected. As the number of accepted atom moves increases, χ^2 will initially decrease until it reaches an equilibrium value. Thus, the atomic configuration corresponding to the equilibrium should be consistent with the experimental total structure factor within the experimental error. From the equilibrium values of the partial pair distribution function, one can calculate the partial coordination number, partial inter-atomic distance and the bond angle distribution.

EXPERIMENTAL TECHNIQUE

Bulk $Ge_{20}Se_{80}$ chalcogenide was prepared using the melt-quench technique. High purity Ge and Se elements (99.999%) were, weighed according to their atomic percentages, charged into chemically cleaned silica tube and then sealed under vacuum of $\approx 1.33 \times 10^{-3}$ Pa. The ampoule was inserted into a furnace where the temperature was gradually increased to 1300 K at heating rate of 3°–4°/min. To get homogeneous melt, the ampoule was frequently rocked for 24 h inside the furnace at the highest temperature. The quenching was made in ice cold water. The glassy state of the quenched alloy was checked using a Philips (PW-1710) X-ray diffractometer. XRD patterns are recorded at scanning speed of 2.4 deg/min with a graphite monochromator, using CuK_α-line (λ = 1.5418 Å). The experiment was done in the scattering angle range $4° \le 2\theta \le 115°$ in steps of 0.1°, which corresponds to K-range $0.284 \le K \le 6.874$ Å^{-1}. Raman spectra was carried out using the 532 nm line of a diode pumped solid state laser. The scattered light is analyzed with a spectrometer equipped with holographic grating and detected with a Andor Newton CCD camera.

RESULTS AND DISCUSSION

As a starting point, the observed X-ray intensities have been corrected through background subtraction followed by absorption and polarization corrections. The corrected X-ray data are used to calculate the total structure factor [16] as a function of the scattering vector, ($K = 4\pi\sin\theta/\lambda$). As shown in Fig. 1, a first sharp diffraction peak (FSDP) which is commonly observed in covalently bonded materials implies the presence of IRO caused by connecting some of the structural units. In order to determine the position and intensity of the pre-peaks, the $S(K)$ spectra have been analyzed using two pseudo-Voigt functions [3] for the pre- and first-peaks. The pseudo-Voigt function is linear summation of Lorentzian and Gaussian compo-

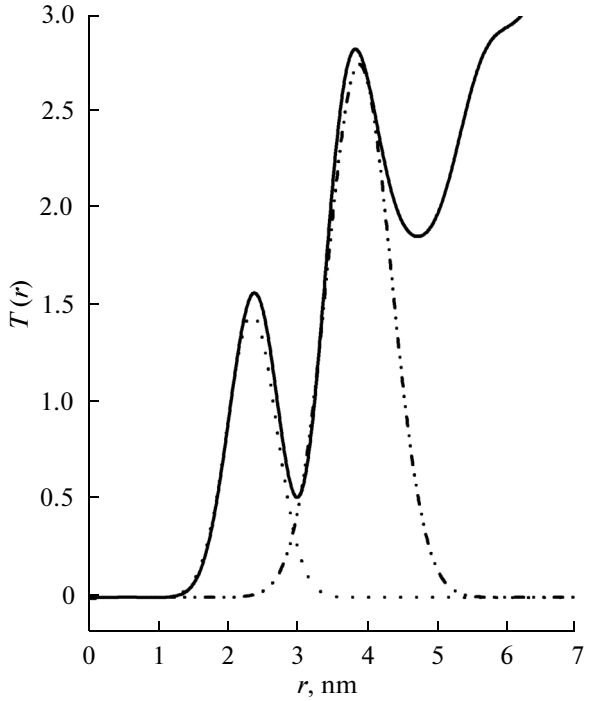

Fig. 3. The total distribution function, $T(r)$, versus r of the studied $Ge_{20}Se_{80}$ glass.

nents [c.Gauss. + (1 – c) Lorent.], where the Gaussian fraction has a value in the range $0 \le c \le 1.0$. The values of the characteristic length ($R = 2\pi/K_0$, where K_0 is the peak position) and the coherence length ($L = 2\pi/\Delta K$, where ΔK is the half-width at half-maximum of the peak), as calculated from the well-resolved FSDP following the procedures published by authors [20], are 5.45 ± 0.05 Å and 17.44 ± 0.52 Å, respectively.

The reduced distribution function, $G(r)$, calculated after one damping correction followed by several Kaplow iterations [21], is shown in Fig. 2. At small values of $r \le 1.5$ Å (see Eq. (2)), $G(r)$ function shows a straight line with slope $= -4\pi\rho_0$. The bulk density obtained from the straight portion of $G(r)$, equals $(3.85 \pm 0.04) \times 10^{-2}$ atom/ Å^3. The bulk density can also be calculated from the relation $\rho_0 = N_A \sum_i x_i d_i / A_i$, where d_i, A_i and N_A are the density, atomic weight of the element i and Avogadro number, respectively [22]. The excellent coincidence between the former value of the bulk density and the calculated one ($\rho_0 = 3.8505 \times 10^{-2}$ atom/Å^3) confirms the high quality of the present glass. The radial distribution function, RDF(r), is shown also in Fig. 2. At high values of r, the curves should fit the parabola, $RDF(r) = 4\pi r^2 \rho_0$. The broadening appeared in the $RDF(r)$ peaks is expected to cause significant errors in determining the short-range order parameters. So instead of $RDF(r)$, the total distribution function, $T(r) = RDF(r)/r$, is commonly used to get the SRO parameters [16]. The sharpness of the $T(r)$ peaks shown in Fig. 3 is much better than that appeared in the $RDF(r)$ curve. Gaussian fit of $T(r)$ curve shown in Fig. 3 has resulted-in two well-resolved peaks, where the positions of the first and second peaks are $r_1 = 2.38$ Å and $r_2 = 3.82$ Å, respectively. These values are in good agreement with those previously obtained by authors [5].

The partial coordination numbers of the $Ge_{20}Se_{80}$ glass as obtained from RMC, CONM and from other references [20, 21]

	Ge–Ge	Ge–Se	Se–Ge	Se–Se
Present	0.03	4.04	1.01	2.26
CONM	0	4	1	1
Ref. [20]	0.22	3.61	0.9	1.71
Ref. [21]	0.22	3.61	0.9	1.71

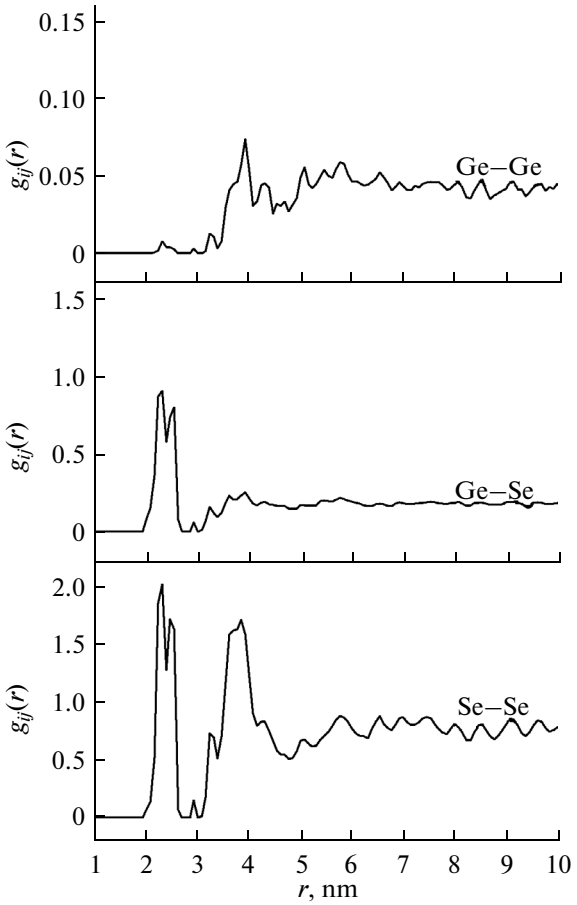

Fig. 4. The partial pair distribution $g_{Ge-Ge}(r)$, $g_{Ge-Se}(r)$, $g_{Se-Se}(r)$ functions versus r of the investigated $Ge_{20}Se_{80}$ glass.

The starting point in RMC simulation [19] is to randomly generate the configuration distribution of $N = 4000$ atoms inside a cubic box. The length of the cubic configuration is 23.6 Å. According to their

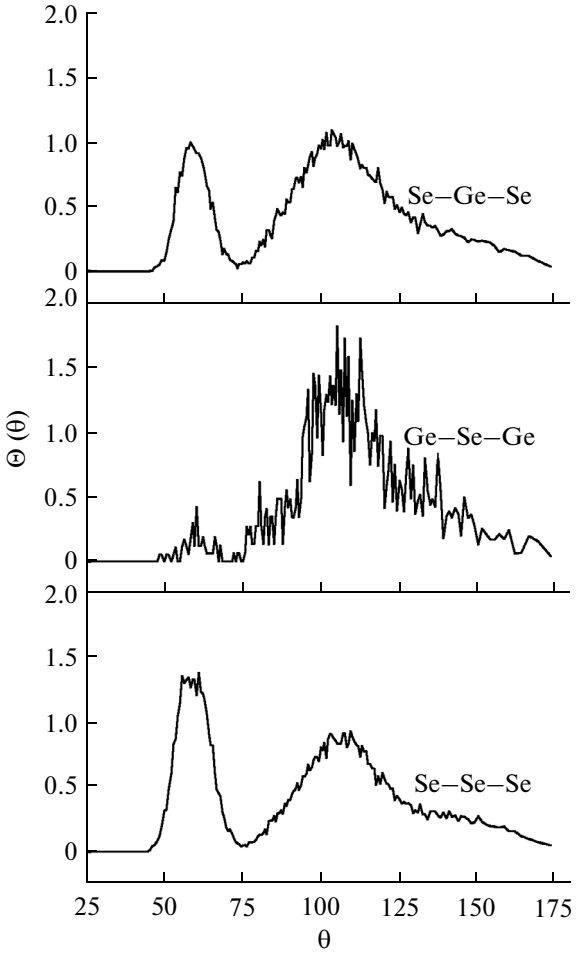

Fig. 5. Bond angle distribution functions, Θ(θ), obtained from RMC simulations.

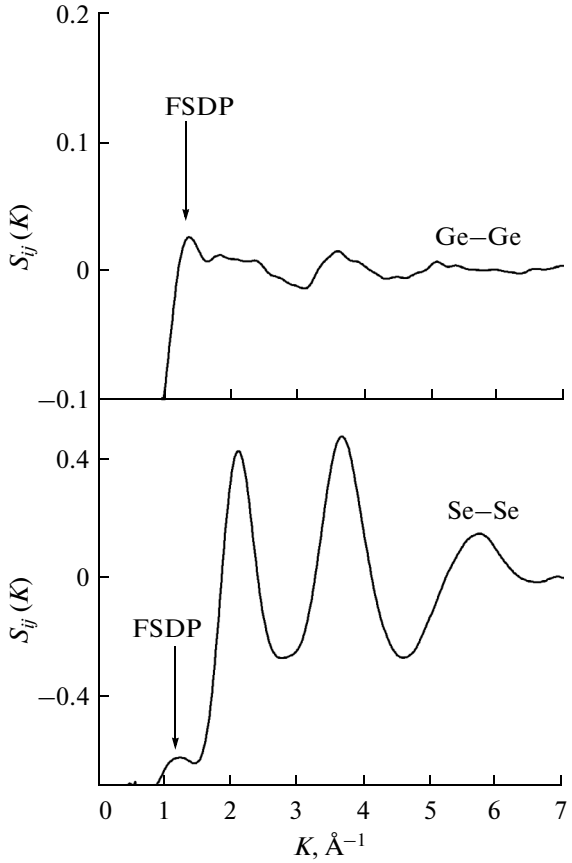

Fig. 6. The partial scattering factors, $S_{ij}(K)$, for the studied $Ge_{20}Se_{80}$ glass.

atomic percentages, the numbers of Ge and Se atoms inside the cube are 800 and 3200 atom, respectively. RMC simulation runs for 20 h using the total structure factor fit under the coordination constraints and a minimum approach distance of 1.96 Å for any atoms pair. When χ^2 oscillates around an equilibrium value, a three-dimensional molecular image of a disordered structure can be obtained. In order to get an accurate image, the average of five simulation trials was taken. Figure 4 shows the partial pair distribution $g_{Ge-Ge}(r)$, $g_{Ge-Se}(r)$, $g_{Se-Se}(r)$ functions. In fact, most of the important structural parameters such as the coordination number, inter-atomic distance and bond angle distribution can be obtained from the partial pair distribution functions. In the first coordination sphere, the near-zero value of $g_{Ge-Ge}(r)$ indicates that only homopolar Se–Se bonds exist in addition to heteropolar Ge-Se bonds. The average Ge–Ge, Ge–Se and Se–Se bond lengths are, as obtained from the refined RMC model, 2.52 ± 0.065, 2.43 ± 0.065 and 2.47 ± 0.065 Å, respectively. The average partial coordination numbers, listed in table, are close to some extent to those reported by other references [4, 6]. Based on the chemical order network model (CONM), the partial coordination numbers are calculated and listed also in table. The presence of Se–Se bridges between the tetrahedral units is a possible reason for high partial coordination number for Se–Se as compared to that reported previously or computed from the chemically ordered network model.

Bond angle distribution functions, Θ(θ), are obtained from the final configuration of the investigated glass using triplets program [6]. In which, the bond angle for any reference atom can be calculated from the cartesian coordinates of the final positions of the surrounding atoms. The Θ(θ) functions of the $Ge_{20}Se_{80}$ glass are shown in Fig. 5. $\Theta_{Se-Ge-Se}(\theta)$ function presents a main peak around 104.2°, which is close to the ideal tetrahedral angle of 109°. A small peak appears at 60° can be attributed to the existence of what we can call it as wrong (homo) bonds. During the melt-quench process, the freeze of Ge atoms in some corner positions of the tetrahedral units instead of Se atoms could be responsible for the above small peak. A reverse behavior is given by $\Theta_{Se-Se-Se}(\theta)$ function, where a main peak is located at 60° and a small one at 104.2°. Selenium atoms occupying face of a

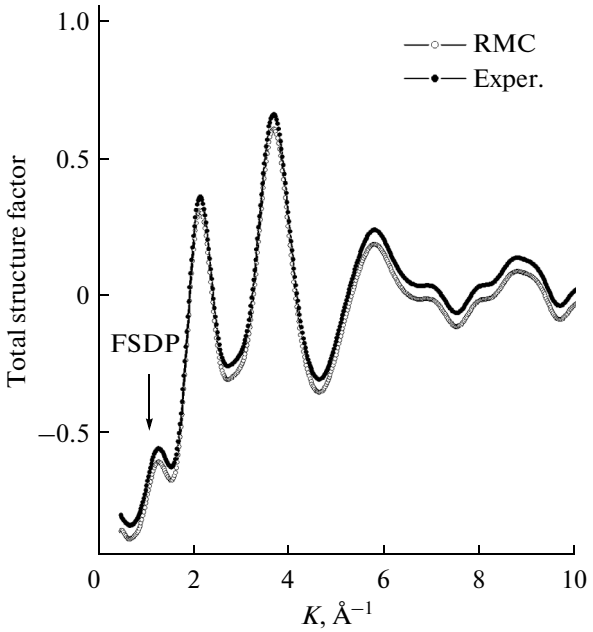

Fig. 7. Experimental scattering factor together with RMC simulation of the studied $Ge_{20}Se_{80}$ glass. RMC data are shifted downward (–0.05) to clarify the coincidence.

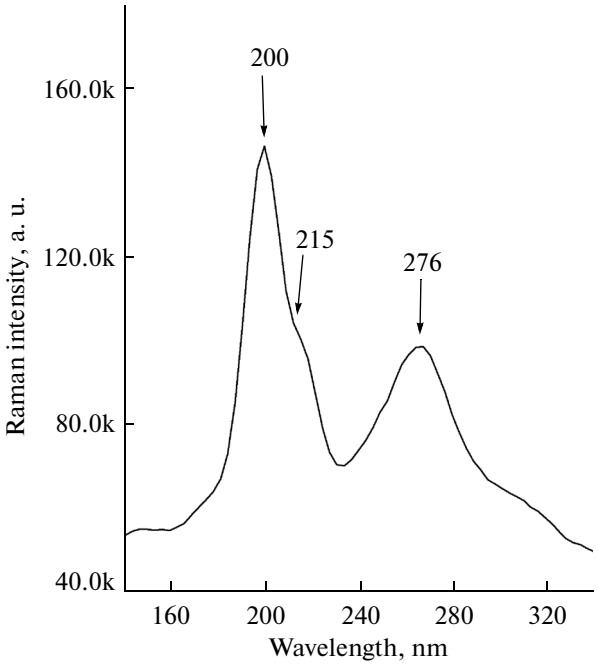

Fig. 8. Raman intensity versus Raman frequency of the investigated $Ge_{20}Se_{80}$ glass.

perfect tetrahedron should exhibit internal angles of 60°. The presence of a $\Theta_{Se-Se-Se}(\theta)$ peak at 104.2° can be attributed to inter-tetrahedral units. The above bond angle distributions can strongly confirm that distorted tetrahedral units in addition to the ideal units are formed inside the cube. These structural units seem to be connected by Se–Se bridges, forming small chains and rings, as previously reported [22]. In the same figure, $\Theta_{Ge-Ge-Ge}(\theta)$ function shows a broad distribution from 50° to 150°, which indicates that pairs of tetrahedral units can be connected either by corner share or edge share.

Fourier transformation of the partial pair distribution gives the corresponding partial scattering factor. The dependence of the partial scattering factors on the scattering vector (K) are shown in Fig. 6. The partial $S(K)$ are important especially in regions where the FSDP is located. Because of its insignificant contribution to the pre-peak, $S_{Ge-Se}(K)$ function is not shown. It was previously mentioned [23] that the pre-peak is originated by Ge–Ge correlation, which bridging $GeSe_{4/2}$ tetrahedra. Recently, the authors [6] have used the reverse Monte Carlo (RMC) simulations and noticed the existence of large number of Se-Se pairs in the first coordination shell suggesting that the tetrahedral units are linked by Se-Se bridges. The FSDP appeared in the partial $S_{Ge-Ge}(K)$ and $S_{Se-Se}(K)$ functions indicate that the intermediate range order is not only attributed to Ge–Ge bonds but also to the presence of Se–Se bonds. Summation of the partial scattering factors gives the total RMC scattering factor as a function of the scattering vector. Figure 7 shows a very good coincidence between RMC simulation and the experimental scattering factor to the point no one can distinguish between their values. In the above figure, the RMC curve is shifted downward by 0.05 in order to differentiate between their values.

Based on the present IRO and SRO parameters, some conclusions about the structural correlations inside the glass matrix are assumed. To confirm such conclusions, Raman spectra measurements of the investigated glass is made and shown in Fig. 8. Two broad as well as one side (shoulder) peaks have appeared. One of the main peaks located at 267 cm^{-1} is related to Se–Se pairs. The second main peak located at 200 cm^{-1} is assigned to the stretching mode of the corner-sharing (CS) $GeSe_{4/2}$ tetrahedra. The latter peak is accompanied by a shoulder at 215 cm^{-1}, which rises from the vibrations of Se atoms in the four member rings composed of two edge-sharing (ES) tetrahedra [24]. The intensities difference between the peak and its shoulder clarify that the studied glass has a lot of CS tetrahedra and few ES tetrahedra.

CONCLUSIONS

The first sharp diffraction peak (FSDP) appeared in the structure factor curve implies the presence of IRO caused by connecting some of the structural units. The values of r_1/r_2 ratio and the corresponding bond angle (Θ), obtained from the conventional (Fourier) method, indicate that the structural units inside the present alloy are $Ge(Se_{½})_4$ tetrahedra connected by

chains of the chalcogen atoms. Reverse Monte Carlo (RMC) simulations of the X-ray scattering data are useful to compute the partial pair distribution functions, $g_{ij}(r)$, the partial structure factors, $S_{ij}(K)$, and consequently the total structure factor. The partial structure factors have shown that not only the homopolar Ge–Ge bonds, but also Se–Se bonds are behind the appearance of the first sharp diffraction peak (FSDP) in the total structure factor. The presence of the tetrahedral $Ge(Se_{½})_4$ structural units which connected by Se–Se chains have been confirmed by the simulated values of the partial coordination numbers and the bond angle distributions. Finally, Raman spectra measurements have strongly supported the conclusions obtained either from the calculated Fourier data or from RMC simulations.

ACKNOWLEDGMENTS

This Project was funded by the Deanship of Scientific Research (DSR), King Abdulaziz University, Jeddah, under grant No. (4/662/D1432). The authors, therefore, acknowledge with thanks DSR technical and financial support.

REFERENCES

1. Inam, F., Shatnawi, M.T., Tafen, D., Billinge, S.J.L., Chen, P., and Drabold, D.A., An intermediate phase in Ge_xSe_{1-x} glasses: Experiment and simulation, *J. Phys.: Condens. Matter*, 2007, vol. 19, no. 45, p. 455206.
2. Sharma, D., Sampath, S., Lalla, N.P., and Awasthi, A.M., Mesoscopic organization and structural phases in network-forming Ge_xSe_{1-x} glasses, *Physica B* (Amsterdam), 2005, vol. 357, pp. 290–298.
3. Wang, Y., Ohata, E., Hosokawa, S., Sakurai, M., and Matsubara, E., Intermediate-range order in glassy Ge_xSe_{1-x} around the stiffness transition composition, *J. Non-Cryst. Solids*, 2004, vol. 337, no. 1, pp. 54–61.
4. Tafen, D. and Drabold, D.A., Models and modeling schemes for binary IV–VI glasses, *Phys. Rev. B: Condens. Matter*, 2005, vol. 71, no. 5, pp. 54206–54220.
5. Rao, N.R., Krishna, P.S.R., Basu, S., Dasannacharya, B.A., Sangunni, K.S., and Gopal, E.S.R., Structural correlations in Ge_xSe_{1-x} glasses—A neutron diffraction study, *J. Non-Cryst. Solids*, 1998, vol. 240, nos. 1–3, pp. 221–231.
6. Machado, K.D., de Lima, J.C., Campos, C.E.M., Gasperini, A.A.M., de Souza, S.M., Maurmann, C.E., Grandi, T.A., and Pizani, P.S., Reverse Monte Carlo simulations and Raman scattering of an amorphous GeSe alloy produced by mechanical alloying, *Solid State Commun.*, 2005, vol. 133, no. 6, pp. 411–416.
7. Hosokawa, S., Wang, Y., Sakurai, M., Bèrar, J.-F., Pilgrim, W.-C., and Murase, K., Rigidity transitions and intermediate structures of Ge–Se glasses—An anomalous X-ray scattering study, *Nucl. Instrum. Methods Phys. Res., Sect. B*, 2003, vol. 199, pp. 165–168.
8. Gulbrandsen, E., Johnsen, H.B., Endregaard, M., Grande, T., and Stølen, S., Short-range order in Se-rich Ge–Se glasses—An EXAFS study, *J. Solid State Chem.*, 1999, vol. 145, pp. 253–259.
9. Susman, S., Price, D.L., Volin, K.J., Dejus, R.J., and Montague, D.G., Intermediate-range order in binary chalcogenide glasses: The first sharp diffraction peak, *J. Non-Cryst. Solids*, 1988, vol. 106, pp. 26–29.
10. Salmon, P.S. and Petri, I., Structure of glassy and liquid $GeSe_2$, *J. Phys.: Condens. Matter*, 2003, vol. 15, no. 16, pp. S1509–S1528.
11. Warren, B.E., Krutter, H., and Morningstar, O., Fourier analysis of X-ray patterns of vitreous SiO_2 and B_2O_2, *J. Am. Ceram. Soc.*, 1936, vol. 19, nos. 1–12, pp. 202–206.
12. McGreevy, R.L., Reverse Monte Carlo modelling, *J. Phys.: Condens. Matter*, 2001, vol. 13, pp. R877–R913.
13. McGreevy, R.L. and Pusztai, L., Reverse Monte Carlo simulation: A new technique for the determination of disordered structures, *Mol. Simul.*, 1988, vol. 1, no. 6, pp. 359–367.
14. Faber, T.E. and Ziman, J.M., A theory of the electrical properties of liquid metals, *Philos. Mag.*, 1965, vol. 11, no. 109, pp. 153–173.
15. Elliott, S.R., *Physics of Amorphous Materials*, 2nd ed. New York: Longman, 1990.
16. Moharram, A.H. and Abdel-Basit, A.M., Structural correlations of AsGeSe glasses, *Physica A* (Amsterdam, Neth.), 2005, vol. 358, nos. 1–4, pp. 279–284.
17. Szczygielska, A., Burian, A., Dore, J.C., Honkimäki, V., and Duber, S., Local structure of saccharose- and anthracene-based carbons studies by wide-angle high-energy X-ray scattering, *J. Alloys Compd.*, 2004, vol. 362, nos. 1–2, pp. 307–313.
18. Keen, D.A. and McGreevy, R.L., Structural modelling of glasses using reverse Monte Carlo simulation, *Nature* (London), 1990, vol. 344, pp. 423–425.
19. http://wwwisis2.isis.rl.ac.uk/rmc.
20. Johnson, R.W., Price, D.L., Susman, S., Arai, M., Morrison, T.I., and Shenoy, G.K., The structure of silicon-selenium glasses: I. Short-range order, *J. Non-Cryst. Solids*, 1986, vol. 83, pp. 251–271.
21. Kaplow, R., Strong, S.L., and Averbach, B.L., Radial density functions for liquid mercury and lead, *Phys. Rev.*, 1965, vol. 138, no. 5A, pp. A1336–A1345.
22. Machado, K.D., de Lima, J.C., Campos, C.E.M., Grandi, T.A., and Pizani, P.S., Reverse Monte Carlo simulations and Raman scattering of an amorphous $GeSe_4$ alloy produced by mechanical alloying, *J. Chem. Phys.*, 2004, vol. 120, no. 1, pp. 329–336.
23. Fuoss, P.H., Eisenberger, P., Warburton, W.K., and Bienestock, A., Application of differential anomalous X-ray scattering to structural studies of amorphous materials, *Phys. Rev. Lett.*, 1981, vol. 46, no. 23, pp. 1537–1540.
24. Dwivedi, P.K., Tripathi, S.K., Pradhan, A., Kulkarni, V.N., and Agarwal, S.C., Raman study of ion irradiated GeSe films, *J. Non-Cryst. Solids*, 2000, vol. 266.